coatings

MDPI

Article

Investigation of the Effects of Component Ratios on the Properties of Superhydrophobic Polyurethane/Fluorinated Acrylic Co-Polymer/SiO_2 Nanocomposite Coatings

Chong Ke [1,†], Zhongfa Li [1,2,†], Chenhua Zhang [1], Xinguo Wu [1], Zhiping Zhu [2,*] and Yongdong Jiang [1,*]

1 Tsinghua Innovation Center in Dongguan, Dongguan 523808, China; kech@tsinghua-dg.org (C.K.); zhongfazfli@163.com (Z.L.); zhangch@tsinghua-dg.org (C.Z.); wuxg@tsinghua-dg.org (X.W.)
2 School of Chemistry and Food Engineering, Changsha University of Science and Technology, Changsha 410000, China
* Correspondence: zzp8389@163.com (Z.Z.); jiangyd@tsinghua-dg.org (Y.J.)
† C.K. and Z.L. contributed equally to this work.

Abstract: In this work, polyurethane/fluorinated acrylic co-polymer/silicon dioxide (PU/FAP/SiO_2) hybrid superhydrophobic coatings were fabricated on glass substrates via a simple one-step coating process. The effects of each coating component on the coating properties were systematically investigated. The optimized coating exhibits a water contact angle (WCA) of 159° and a rolling angle of 3°. Meanwhile, the coating has an optical light transmittance of 88%, indicating the good transparency of the coating. Besides, the coating demonstrates an adequate level of abrasion resistance. After a total abrasion distance of 300 cm against a piece of 800 mesh sand paper, the sample still kept a water contact angle of about 110°, showing its high abrasion resistance. Therefore, the optimized coating has a great potential for practical application.

Keywords: superhydrophobic; nanocomposite; polyurethane; SiO_2; transparent

check for updates

Citation: Ke, C.; Li, Z.; Zhang, C.; Wu, X.; Zhu, Z.; Jiang, Y. Investigation of the Effects of Component Ratios on the Properties of Superhydrophobic Polyurethane/Fluorinated Acrylic Co-Polymer/SiO_2 Nanocomposite Coatings. *Coatings* **2021**, *11*, 174. https://doi.org/10.3390/coatings11020174

Academic Editor: Nicolas Delorme
Received: 27 December 2020
Accepted: 28 January 2021
Published: 2 February 2021

Publisher's Note: MDPI stays neutral with regard to jurisdictional claims in published maps and institutional affiliations.

Copyright: © 2021 by the authors. Licensee MDPI, Basel, Switzerland. This article is an open access article distributed under the terms and conditions of the Creative Commons Attribution (CC BY) license (https://creativecommons.org/licenses/by/4.0/).

1. Introduction

Inspired by the unique water repelling nature of lotus leaves, superhydrophobic surfaces have been extensively explored for various potential applications, such as anti-fogging, anti-icing, anti-corrosion, oil/water separation, self-cleaning and anti-contamination, etc. [1–7]. Superhydrophobic surface has a water contact angle (WCA) higher than 150° and a water rolling angle less than 10°. In general, the superhydrophobic surfaces are fabricated by creating rough surface structures on low surface energy materials or utilizing low surface energy compounds to decorate materials with micro/nano-scale hierarchical rough surfaces [8–10]. To date, superhydrophobic surfaces on different substrates including glass, ceramics, metals, polymers, fabrics and etc.,have been fabricated through various techniques, such as chemical etching, sol-gel, spraying, dip-coating, spin-coating, chemical vapor deposition and thermal oxidation [11–15]. Nevertheless, the superhydrophobic surfaces are vulnerable when working at high temperatures, in acid/alkali solutions, and under ultraviolet radiation and often of low abrasion resistance, which limits the practical applications of superhydrophobic coatings [16]. Therefore, it is extremely important to design and fabricate high performance superhydrophobic coatings with prolonging lifetime under various harsh working conditions.

It has been reported that polymers with low surface energy, such as polyacrylate (PA) [17,18], polystyrene (PS) [19,20], polyvinylidene fluoride (PVDF) [21,22], poly(dimethylsiloxanes) (PDMS) [23,24], epoxy [25,26], poly(methacrylic acid) (PMAA) [27,28], polyurethane (PU) [29–31], and have been used to fabricate superhydrophobic coatings. However, the water contact angle of these polymers is generally less than 120° on a homogeneous flat surfaces. The incorporation of inorganic nanoparticles, such as SiO_2 [32,33], TiO_2 [34,35] and ZnO [36,37], can increase the surface roughness of the hydrophobic coatings, therefore, their contact angles, based on the Wenzel and Cassie-Baxter models, which show excellent water repellence and superhydrophobicity. For example, Satapathy et al. [38] prepared linear low density polyethylene (LLDPE)/SiO_2 superhydrophobic nanocomposite coatings by dip-coating technique. The porosity of the coatings was controlled by using phase separation method, the addition of non-solvent ethanol causes phase separation, in which a portion of LLDPE precipitates from the polymer matrix. With more non-solvent ethanol added into the system, more LLDPE precipitates from the polymer matrix, which increases the porosity of the coating. The coating's WCA was 170° and the sliding angle was 3.8°. Besides, the coatings exhibit good thermal stability and durability as well. Radwan et al. [39] fabricated poly vinylidene fluoride (PVDF)/ZnO superhydrophobic composite coating on Al substrate. The coating shows a WCA of 155° and a WCA hysteresis of 4.5° with good corrosion protection property.

Among various polymers used to prepare superhydrophobic coatings, such as PA, PS, PVDF, PDMS, etc. Polyurethane is considered as one of the promising candidates due to its good optical transparency, stable weatherability and superior mechanical property.

Zheng et al. [31] prepared PMMA-fluorinated SiO_2 nanoparticle double layer composite coatings by a two-step spraying deposition method. Firstly, a layer of car refinishing paint was spray on the substrate, and the sample was dried at ambient temperature for 5 min. Subsequently, the PMMA-fluorinated SiO_2 nanocomposite coating was sprayed on the sample. Afterwards, the sample was dried at ambient temperature for 2 h to remove any ethanol and water. Although the coating exhibits superhydrophobicity and good abrasion resistance, the optical light transmittance of the composite coating is lower than 80%. In a report by Luo et al. [29], SiO_2 nanoparticle dispersion was firstly prepared by a sol-gel method using methyltrimethoxysilane as precursor and methanol as solvent in the presence of oxalic acid and NH_4OH as catalyst. Then a two-step dip-coating technique was employed to fabricate the PU/SiO_2 double layer composite coating by dipping glass slide in PU solution and SiO_2 nanoparticle dispersion. Excellent performance, with a WCA of 162° and a transmittance of 90%, was achieved. However, the process was complex and time consuming. Although significant progress has been made in fabrication of superhydrophobic coatings recently, problems including complex preparation process, harmful reagents used and poor transparency, abrasion resistance and hardness, which limit practical applications of superhydrophobic coatings, remain unsolved. Moreover, for composite coatings, understanding the effects of different components on the coating properties is important for the development of superhydrophobic composite coatings. However, few systematic studies in this field was reported. Moreover, it has been reported that such composite coatings can not only change the wettability of the surface, but also they can induce changes in other properties including thermal and electrical conductivity, which makes them candidates for various applications [40–42].

Herein, we report a facile, one-step dip-coating method to prepare polyurethane/silicon dioxide (PU/SiO_2) superhydrophobic coatings on glass substrates. The hybrid coatings exhibit superhydrophobic property with a WCA of about 159° and a rolling angle of less than 3°. In this work a convenient approach to create a mechanically robust and durable superhydrophobic coating with a proper abrasion resistance was developed. More importantly, the influences of the different coating constituents, including PU, ST-200 and SiO_2 nanoparticles on surface morphology, hydrophobicity and optical transmittance, were systematically studied.

2. Materials and Methods

2.1. Materials

FAP dispersion (Capstone™ ST-200) was purchased from Guangzhou Jianyi Chemical Import and Export Co., Ltd., Guangzhou, China. SiO_2 nanoparticles, AEROSIL R812s with a specific surface area of 195–245 m^2/g were obtained from Evonik Co., Ltd. Hanau, Germany. Solvent-based polyurethane resin (PU-166), serving as a binder and host for the SiO_2 nanopartices, was purchased from Anhui Sinograce Chemical Co., Ltd., Hefei, China. Butanone and toluene were supplied by Dongguan Jiabao Petrochemical Co., Ltd., Dongguan, China. Adhesion promoter (BYK-4510) was received from Jiangmeng Dongyang Chemical Co. Ltd. Jiangmen, China. The glass substrates with a size of 90 mm $\times$ 90 mm $\times$ 2 mm were ordered from GULUO Glass Luoyang, China.

2.2. Coating Preparation

Certain amount of the R812s SiO_2 nanoparticles was first dispersed in a solvent mixture of butanone and toluene (with a volume ratio of 50:50) by ultrasonication for 30 min. Secondly, the Capstone™ ST-200 FAP and PU-166 polyurethane (PU) were added to the prepared SiO_2 nanoparticle suspension and mechanically stirred for 30 min. Afterwards, the adhesion promoter BYK-4510 was added and stirred mechanically for another 30 min to form a uniform coating solutions.

Before preparing the coating samples, glass substrates were cleaned in acetone, ethanol, and deionized water, respectively, for 10 min, and followed by drying in an oven at 80 °C for 30 min. The composite coatings were fabricated on the glass substrates via a dip coating method, in which the cleaned glass substrates were dipped in the coating solutions and drawn at a speed of 2 cm/s. Finally, the coated samples were cured at 100 °C for 1 h.

Three series of samples with varied contents of SiO_2 nanoparticles, PU, and ST-200, respectively, were prepared. The content of the adhesion promoter, BYK-4510, was set at 0.24 wt.% in the coating solution for all the samples. In order to investigate the effects of SiO_2 nanoparticle content on the coating properties, samples with different SiO_2 nanoparticle contents from 0 to 4 g with an increment of 1 g (denoted as sample R0 to R4, e.g., sample R4 was prepared using a solution containing 4 g of SiO_2 nanoparticles every 100 g solution) were prepared. For these samples, the PU was 5.0 wt.% while ST-200 was 2.5 wt.% in the coating solution. Similarly, coating samples with various PU contents from 0 to 10 g (denoted as sample P0 to P10, e.g., sample P5 was prepared using a solution containing 5 g of PU every 100 g solution) and different ST-200 contents from 0 to 10 g (denoted as samples S0 to S10, e.g., sample S5 was prepared using a solution containing 5 g of ST-200 every 100 g solution) were fabricated. For samples with varying PU loadings, SiO_2 nanoparticle was 2.0 wt.% while ST-200 was 2.5 wt.% in solution. For samples with different ST-200 contents, SiO_2 nanoparticle was 2.0 wt.% while PU was 5.0 wt.% in solution.

2.3. Characterization

The coating surface morphology was observed by Hitachi SU8000 Scanning Electron Microscopy (SEM) Hitachi High-Tech, Japan. Atomic force microscope (AFM, Oxford Instruments Cypher S) (Oxford Instruments, Abingdon, UK) was utilized to measure the surface roughness of the coating. Static and dynamic water contact angle (WCA) measurements were carried out using a JCY-2 contact angle measuring system (Shanghai Ruifang Instrument, Shanghai, China) by carefully applying water droplets (4 μL) onto sample surfaces. The average WCA was determined by measuring the same sample at three randomly chosen area. The coatings' optical transmittance was tested by a haze meter (WGT-S) (Shanghai Shenguang Instrument, Shanghai, China).

The hardness of the coatings was measured by pencil test based on GB/T 6739 standard, which is conformed to ISO-15184. During the test, sample was placed on a hard and horizontal table surface. The pencil was hold against the coating surface at an angle of 45° and pushed forward for 10 mm at a speed of 1 mm/s. Initially, the pencil with the highest hardness was applied, afterwards, pencils with lower hardness were used in the test until the pencil did not cut through the coating nor scratched the coating surface. And the hardness of the coating was determined by the hardest pencil which did not cut through the coating during the test. The scale of hardness of the pencils ranges from 9B, the softest, to 9H, the hardest.

The adhesion of the coatings to substrates was evaluated by the cross-cut test based on GB/T 9286, which is conformed to ISO-2409. 20 mm long, 10 $\times$ 10 grid lines with 1 mm interspacing were cut by a razor blade on each sample. Then, a piece of 3M 600 tape was applied on the grid area and peeled off. The grid area was finally inspected and adhesion was rated according to the standard. The adhesion rates range from 0 to 5, in which rate 0 means 0% of the coating area is removed during the test.

The mechanical durability of the coatings was analyzed via an abrasion test. In the abrasion test, a load of 200 g was first put on the coating sample (3 cm $\times$ 3 cm), then, the coating sample was dragged on a piece of sandpaper (800 mesh) for 20 cm, which was defined as one abrasion cycle. WCA was measured after each abrasion cycle. The test sample surface was then examined by an optical microscope.

3. Results and Discussion

3.1. Effects of SiO_2 Nanoparticle Loading

To evaluate the effects of different components on the physical properties of the coatings, static WCA and optical transmittance were measured on different specimens. When plotting the relationships between the physical properties and the component ratios of the coatings, the component ratios in the coating solutions were converted to solid component ratios in the coatings. Figure 1 shows the WCA and optical transmittance of the superhydrophobic coatings with different SiO_2 nanoparticle loadings. The PU and FAP ST-200 were 5 and 2.5 wt.%, respectively, in the coating solutions. It is obvious that the WCA of these coatings shows an increasing trend with the increase of the SiO_2 nanoparticle loading (Figure 1a). The sample with 27.9 wt.% SiO_2 nanoparticles has the highest WCA of 153.5°. Further increase of SiO_2 nanoparticles leads to a slight decrease in WCA. Figure 1b shows that the optical transmittance of the coatings decreases with increasing SiO_2 nanoparticle loadings. But all the coatings measured keep an optical transmittance of larger than 77%. The decrease in optical transmittance is mainly attributed to the increased scattering of visible light by more pores and agglomerates with the increase of SiO_2 nanoparticles.

The surface morphologies of the coatings with different SiO_2 nanoparticle loadings were examined by SEM. Figure 2 shows the SEM images of the superhydrophobic coatings with various loadings of SiO_2 nanoparticles. It can be seen that when SiO_2 loading is less than 34.1 wt.%, the SiO_2 nanoparticles are dispersed well in the coatings, without obvious agglomerates formed. With the increase of the SiO_2 nanoparticles in the coatings, the coatings' surface roughness becomes higher and higher. Therefore, their hydrophobicity increases gradually to reach the superhydrophobic state. The combination of low surface energy, which is provided by the component ST-200, and the increased roughness leads to the increased hydrophobicity. However, when SiO_2 loading reaches 34.1 wt.%, larger agglomerates formed (Figure 2f). The formation of these agglomerates has little impact on the hydrophobicity of the coating. In terms of the optical light transmittance, due to the difference of refractive indexes between the SiO_2 nanoparticles and the polymer matrix, the more SiO_2 nanoparticles added, the more light is reflected and scattered, which causes the decreased optical transmittance. In addition, when SiO_2 loading reaches 34.1 wt.%, the formed agglomerates causes more light scattering as well, and hence, a rapid decrease in optical transmittance.

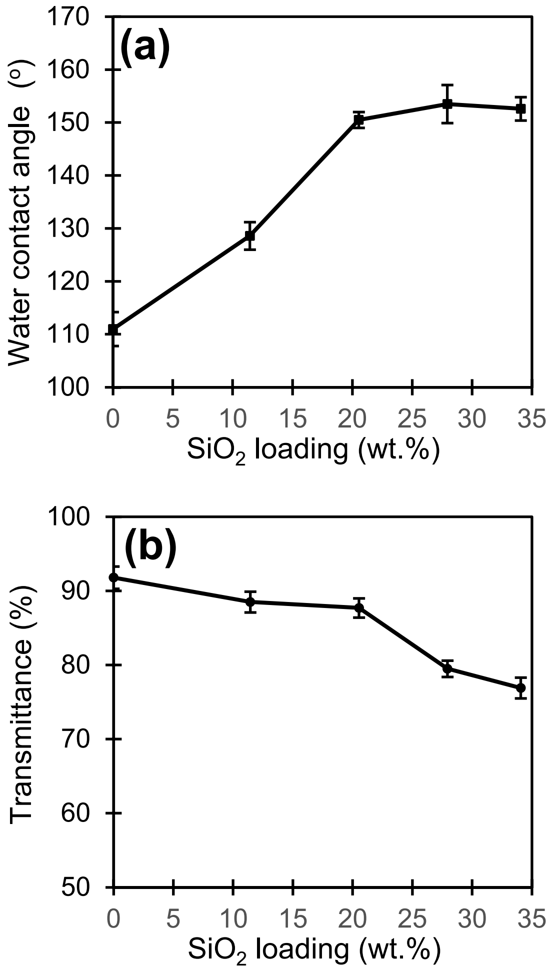

Figure 1. (**a**) WCA and (**b**) optical transmittance of the superhydrophobic coatings with different SiO_2 nanoparticle loadings.

The nanoparticle loading has little impact on the hardness of the coating as all the tested samples present a hardness of 5H or higher. In terms of adhesion strength, with a SiO_2 loading of 27.9 wt.% or lower in the coatings the fabricated coatings have an adhesion rate of 0, which means no coating was peeled off by the adhesion test. These excellent hardness and adhesion imply that these coatings not only have superhydrophobicity, but also high mechanical performance.

In the current coating system, PU mainly functions as a binder and host to hold the SiO_2 nanoparticles and forms continuous coating, which also provides high abrasion resistance. The FAP ST-200 reduces the coatings' surface energy. SiO_2 nanoparticles construct micro-/nanometer hierarchical rough surface structures and increase surface roughness significantly. The combination of high surface roughness and low surface energy leads to the superhydrophobicity of the coatings.

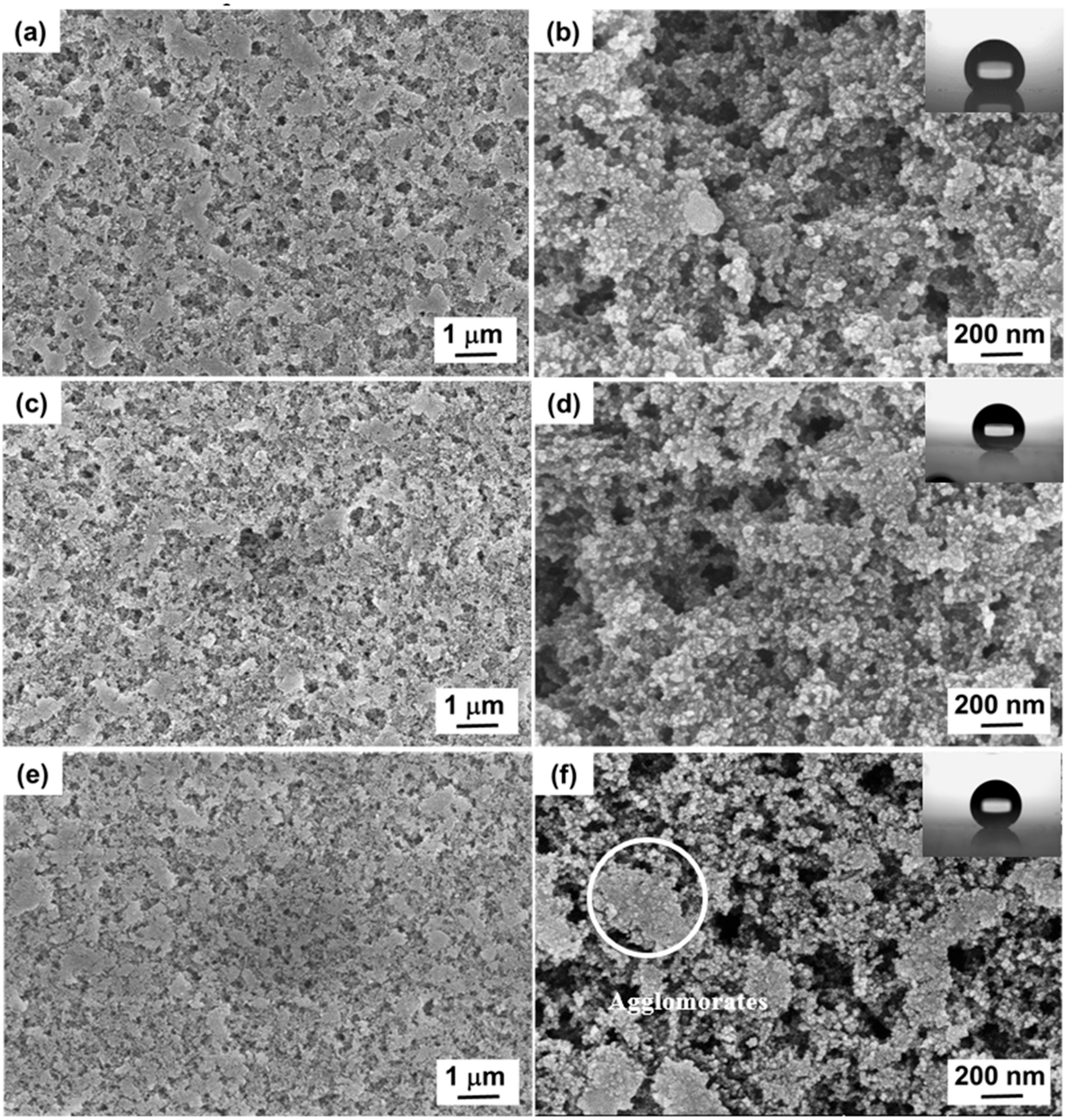

Figure 2. SEM images of the superhydrophobic coatings with different SiO2 nanoparticle loadings, (**a**,**b**) 11.4 wt.%, (**c**,**d**) 20.5 wt.%, (**e**,**f**) 34.1 wt.%, the insets are optical images of water droplets on the specific coatings.

3.2. *Effects of PU Loading*

The effects of PU loading were also studied while ST-200 and SiO_2 nanoparticles were kept at 2.5 and 2.0 wt.%, respectively, in the coating solutions. The WCA and light transmittance of these coatings are present in Figure 3. As shown in Figure 3a, the WCA of these coatings increases slightly with increasing PU loading and reaches the maximum of 158.5° at a PU loading of 45.7 wt.%, while the rolling angle of this sample is about 3°, showing the excellent hydrophobicity of this coating. However, with an excessive amount of PU added, the WCA drops and decreases rapidly from 158.5 o to 112.4° at a PU loading of 67.8 wt.%. Figure 3b demonstrates that the optical transmittance of the superhydrophobic coatings keeps almost the constant and remain higher than 85%, with PU loading up to 55.9 wt.%. Further increasing PU beyond 55.9 wt.%, the optical transmittance is increased gradually and reaches 92% at a PU loading of 67.8 wt.%.

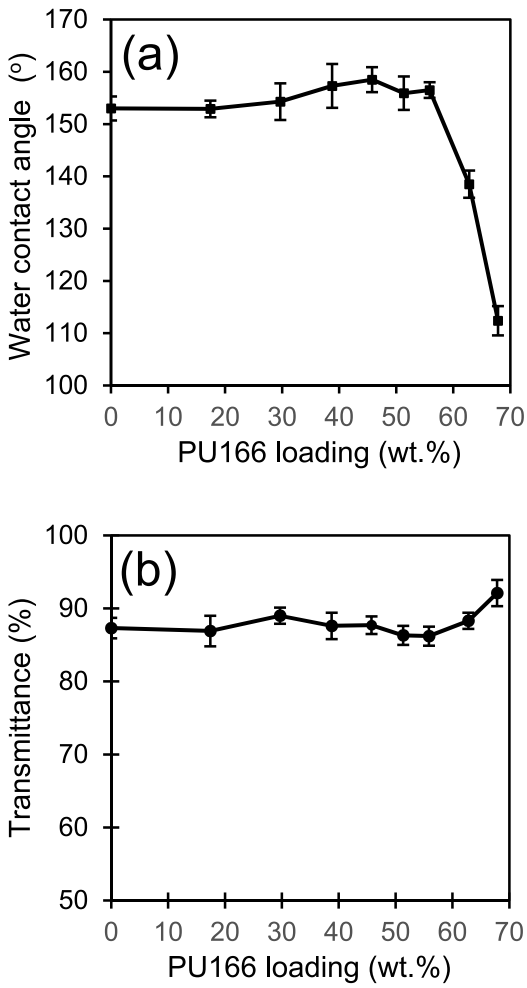

Figure 3. (**a**) WCA and (**b**) optical transmittance of the coatings with different PU loadings.

All the tested samples, but the one without SiO_2 nanoparticles added, have a pencil hardness of 6H or higher. In terms of adhesion, the samples with a PU loading of 45.8 wt.% or higher have an adhesion rate of 0.

To understand the effects of PU on coatings' performance and surface morphologies, SEM images of three coatings with different PU loadings were taken (Figure 4). A porous structure was observed on the sample with 17.4 wt.% PU (Figure 4a). A large amount of SiO_2 nanoparticles can be clearly distinguished at higher magnification (Figure 4b). With more PU added (45.7 wt.%), the SiO_2 nanoparticles are covered partially by PU and the coating still exhibits a porous structure with micro/nano-scale roughness (Figure 4c,d). However, with excessive amount of PU (67.8 wt.%) in the coating, it presents a totally different surface morphology compared to the coatings with lower PU contents. A more flattened structure was observed on the surface (Figure 4e), and only a few nanoparticles can be found on the crack area (Figure 4f). With an excessive amount of PU added in the coating, most of the SiO_2 nanoparticles were covered by PU, therefore, the roughness of the coated surface was significantly reduced. The surface morphology is transformed from a Cassie Baxter state to a Wenzel state. Hence, the hydrophobicity is severely deteriorated.

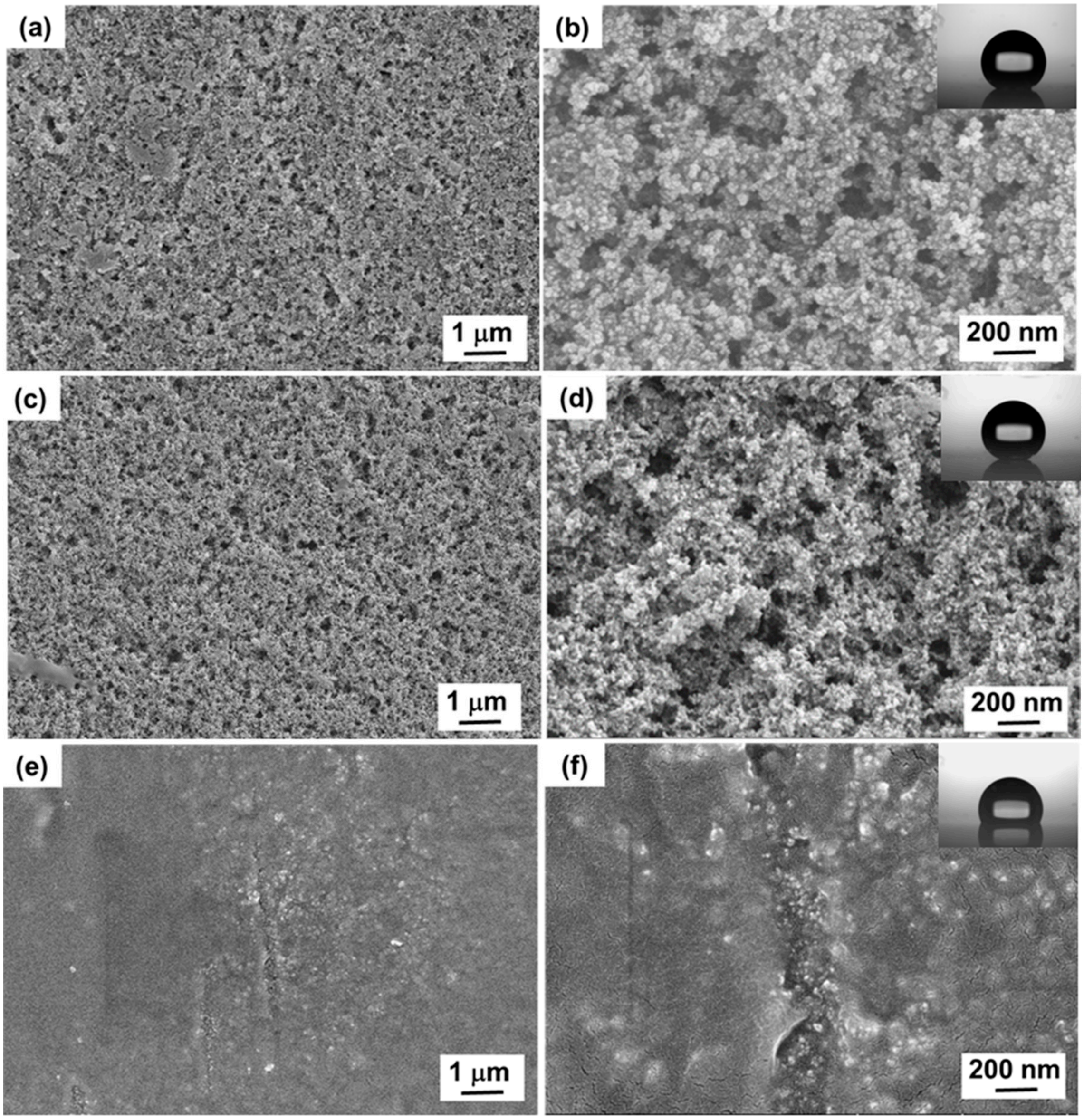

Figure 4. SEM images of the superhydrophobic coatings with different PU166 polyurethane loadings, (**a**,**b**), 17.4 wt.%, (**c**,**d**) 45.8 wt.%, (**e**,**f**) 67.8 wt.%, the insets are optical images of water droplets on the specific coatings.

The surface roughness of coatings with different PU loadings were measured to investigate the impact of surface roughness on the hydrophobicity and transmittance (Figure 5). With a PU loading of 67.8 wt.%, the coating exhibits a flattened surface (Figure 5a) which has a root mean square roughness, R_q, of 24.0 nm, such coating has a WCA of 112.4° and an optical light transmittance of 92.1%. When the PU loading is 62.8 wt.%, the coating presents a rougher surface (Figure 5b) with an R_q of 48.0 nm, such coating exhibits a WCA of 138.5° and an optical light transmittance of 88.3%. A higher roughness results in a better hydrophobicity and lower transparency. For the coating with a PU loading of 45.8 wt.%, the coating exhibits an even rougher surface (Figure 5c), the R_q is 127.0 nm, and such coating has a WCA of 158.5° and an optical light transmittance of 87.7%. It is concluded that the surface roughness has a positive effect on the hydrophobicity but a negative effect on the transparency of the coating.

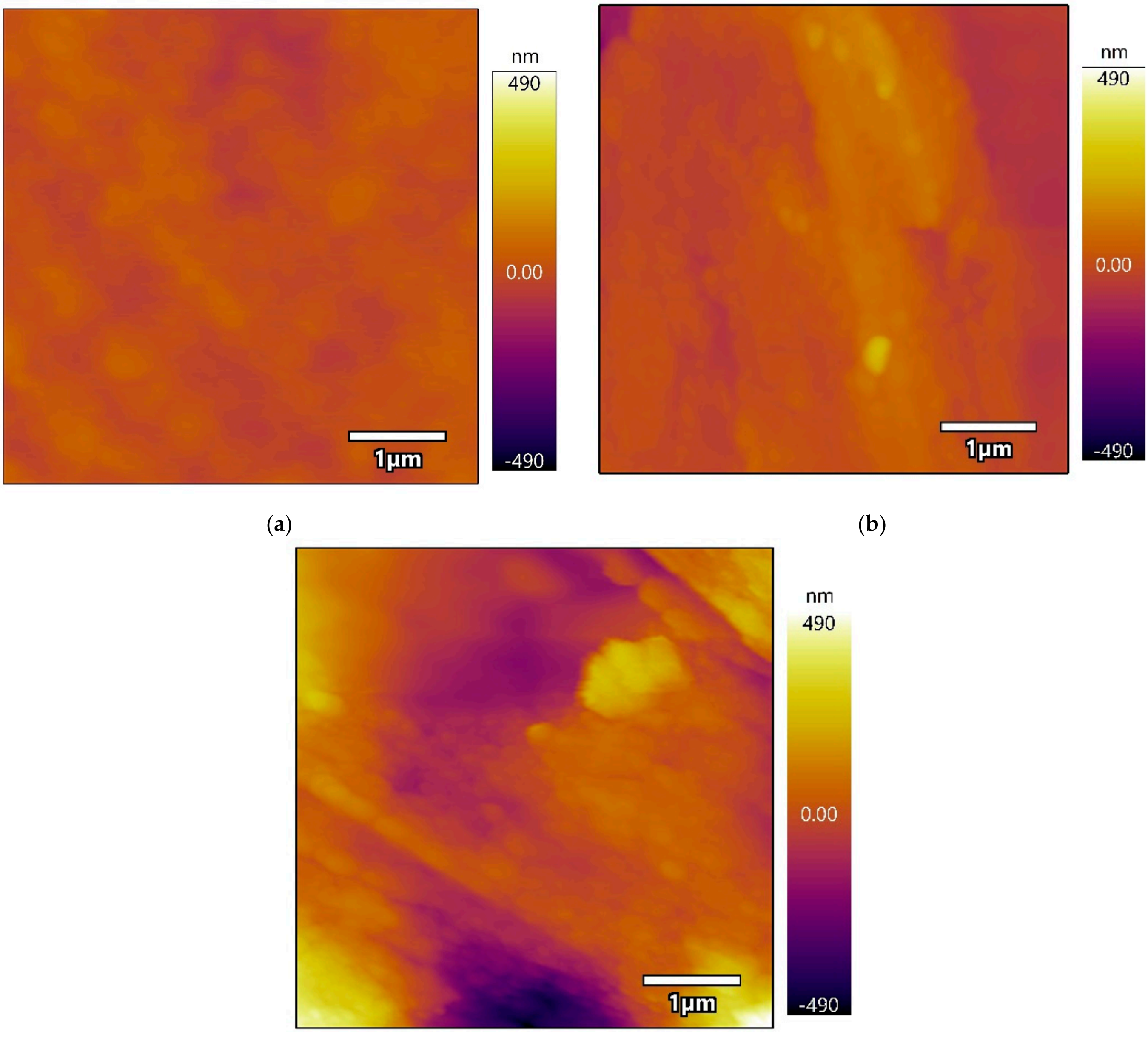

Figure 5. AFM results for coatings with different PU loadings (**a**) 67.8 wt.%, (**b**) 62.8 wt.% and (**c**) 45.8 wt.%.

3.3. Effects of Fluorinated Acrylic Copolymer ST-200

In addition to SiO_2 nanoparticle and PU components, the FAP ST-200 was found to have a significant impact on the physical properties of the composite coatings as well. The relationship between the physical properties of the coatings and the amount of the ST-200 is shown in Figure 6. For these samples, PU and SiO_2 nanoparticles were 5.0 and 2.0 wt.%, respectively, in the coating solutions. As shown in Figure 6a, the WCA increases with the increment of ST-200, until reaching the highest value of 155.8° at a ST-200 loading of 21.6 wt.%. ST-200 is a low surface energy fluorinated polymer. With more and more ST-200 added, the coatings' surface energy becomes lower and lower until it gets close to that of ST-200 itself. Together with the surface roughness created by the SiO_2 nanoparticles, the coatings' hydrophobicity becomes higher and higher. When an excessive ST-200 is added, especially when ST-200 loading is beyond 29.3 wt.%, WCA declines rapidly. However, as plotted in Figure 6b, the optical transmittance of these coatings remains almost the constant, implying that the FAP ST-200 has little effect on coatings' optical property.

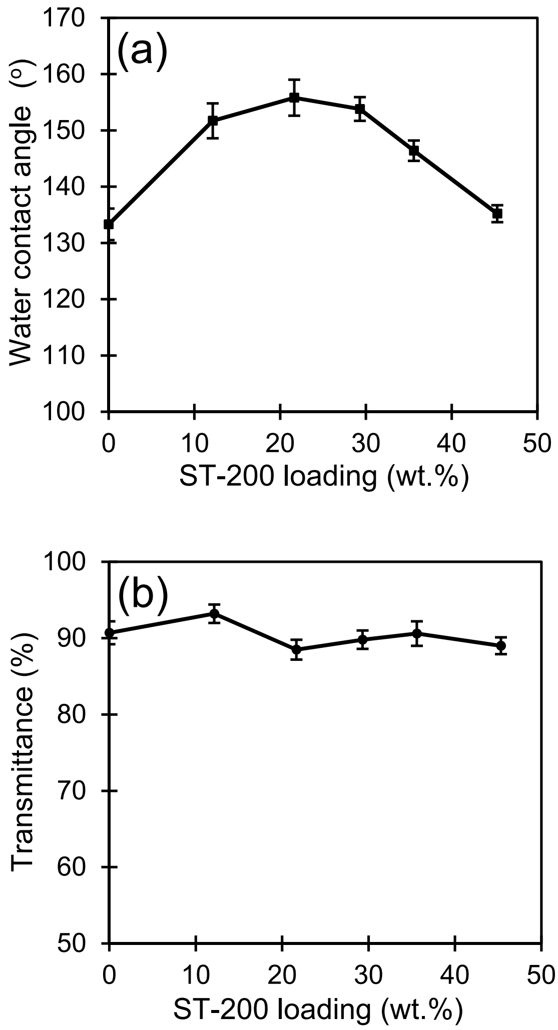

Figure 6. (**a**) WCA and (**b**) optical transmittance of the superhydrophobic coatings with different ST-200 loadings.

All the tested samples have an adhesion rate of 0. The sample with the highest WCA has a pencil hardness of 4H. When ST-200 loading reaches 45.3 wt.% or higher, the coatings' hardness reaches 7H.

The coatings' morphologies with different ST-200 loadings are presented in Figure 7. It is clear that when the ST-200 loading is 21.7 (Figure 7c,d) or 12.1 wt.% (Figure 6a,b), the coatings have a porous structure with micro/nano-scale roughness. With more ST-200 added into the coating, the surface energy of the coating was reduced, which leads to the improved hydrophobicity of the coating. However, when the ST-200 reaches 45.3 wt.% (Figure 7e,f), the surface roughness was reduced, which is due to the fact that most SiO_2 nanoparticles were wrapped and covered by the ST-200. The hydrophobicity of the coating depends on both the appropriate surface roughness and the low surface energy of the coating. In this case, the excessive amount ST-200 added in the coating may reduce the surface energy of the coating, however, the surface roughness was significantly reduced. Therefore, with an excessive amount ST-200 added, the hydrophobicity of the coating is compromised.

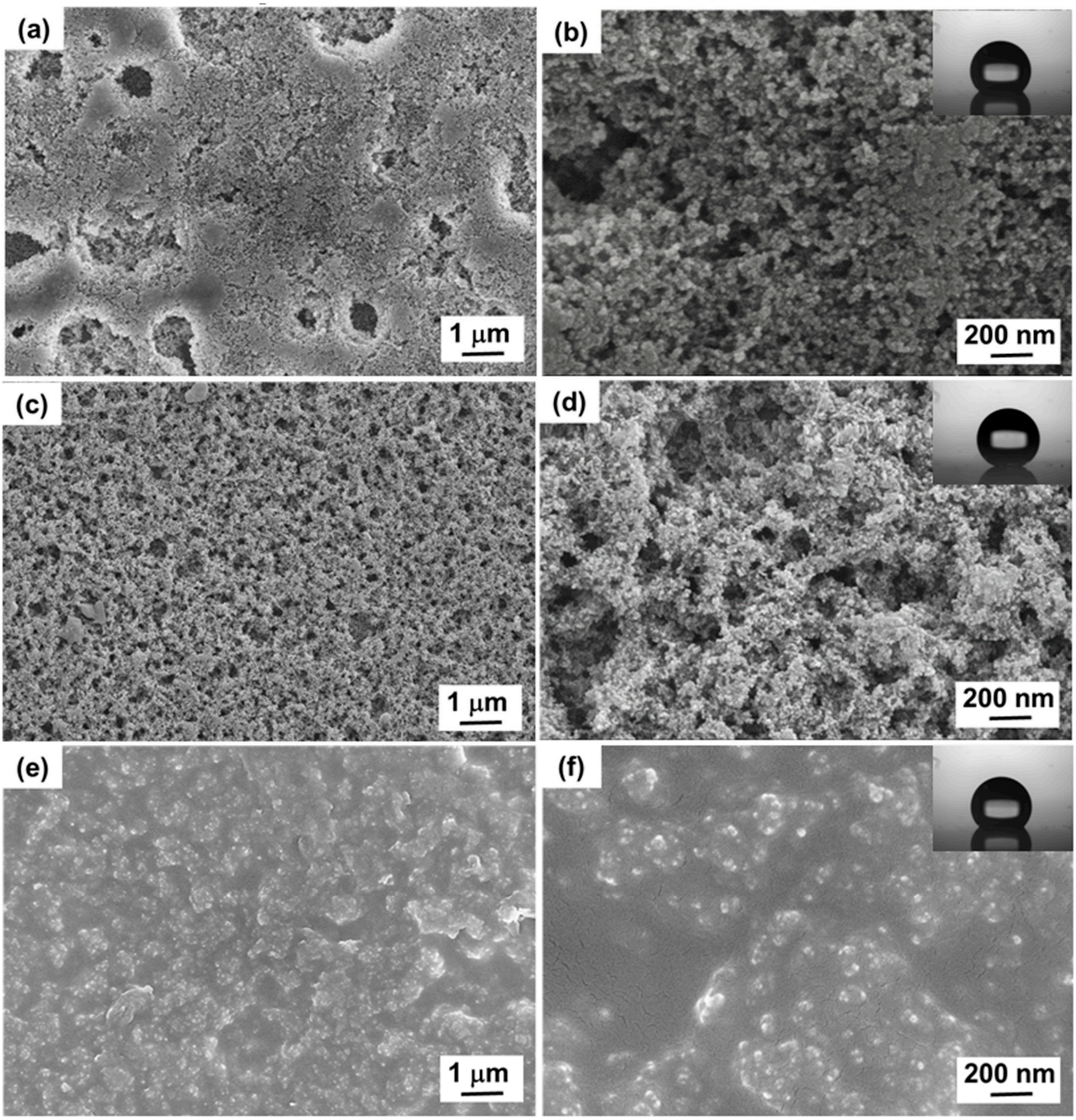

Figure 7. SEM images of the superhydrophobic coatings with different ST-200 loadings, (**a**,**b**) 12.1 wt.%, (**c**,**d**) 21.7 wt.%, and (**e**,**f**) 45.3 wt.%, the insets are optical images of water droplets on the specific coatings.

3.4. Abrasion Resistance

The coating's robustness was examined by an abrasion test, in which a selected coating sample with 45.77 wt.% PU, 28.60 wt.% ST-200 and 22.88 wt.% SiO_2 nanoparticles, was rubbed against a piece of 800-mesh sand paper. The WCA of the sample after each cycle of abrasion is shown in Figure 8. The sample had an initial WCA of about 159°. Its WCA decreased gradually with increasing abrasion cycles. After a total of 25 abrasion cycles, the final WCA of the sample was about 110°, which is still hydrophobic after a total abrasion distance of 300 cm with a weight load of 200 g, showing the high abrasion resistance of this sample.

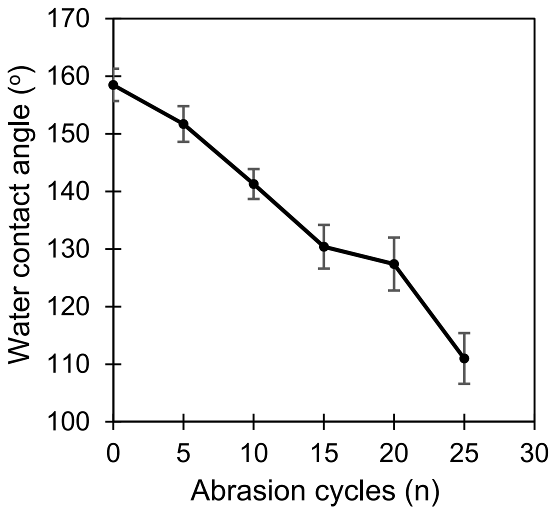

Figure 8. WCA of the tested coating vs. abrasion cycles.

Figure 9 shows the optical images of the rubbed sample before and after the abrasion test. Before the abrasion test the sample had a rough surface with uniform textures. After the abrasion test, scratches formed on the sample surface and its surface roughness was reduced so that its hydrophobicity was decreased significantly.

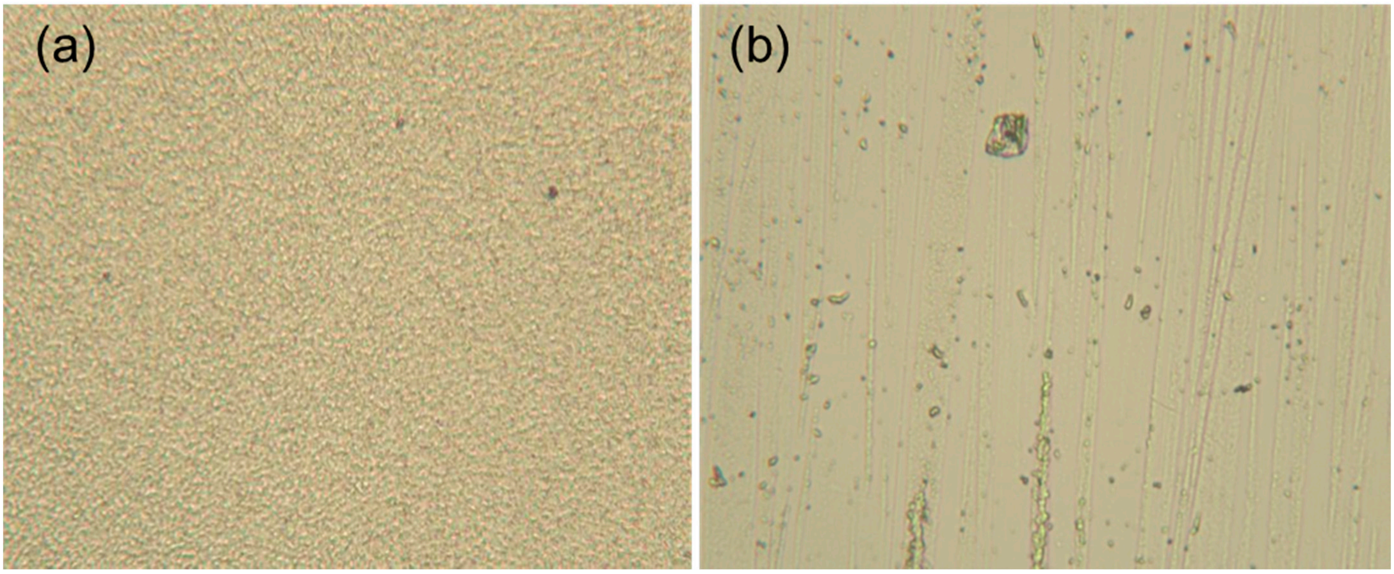

Figure 9. Optical images (200×) of the abrasion tested sample: (**a**) before and (**b**) after 25 abrasion cycles.

3.5. Practical Applications

To evaluate the applicability of these superhydrophobic coatings, the coating solution for the sample with 22.9 wt.% SiO_2 nanoparticle, 45.8 wt.% PU and 28.6 wt.% ST-200, was sprayed onto glass, Al_2O_3 ceramic, fabric and Al substrates. The optical images of water droplets on these samples are shown in Figure 10. It is clear that water droplets on these samples are all close to a sphere and can roll off from the surface easily, showing the high WCA and superhydrophobicity, which implies that the coatings can be applied to a wide range of substrates and have great potential for different application fields.

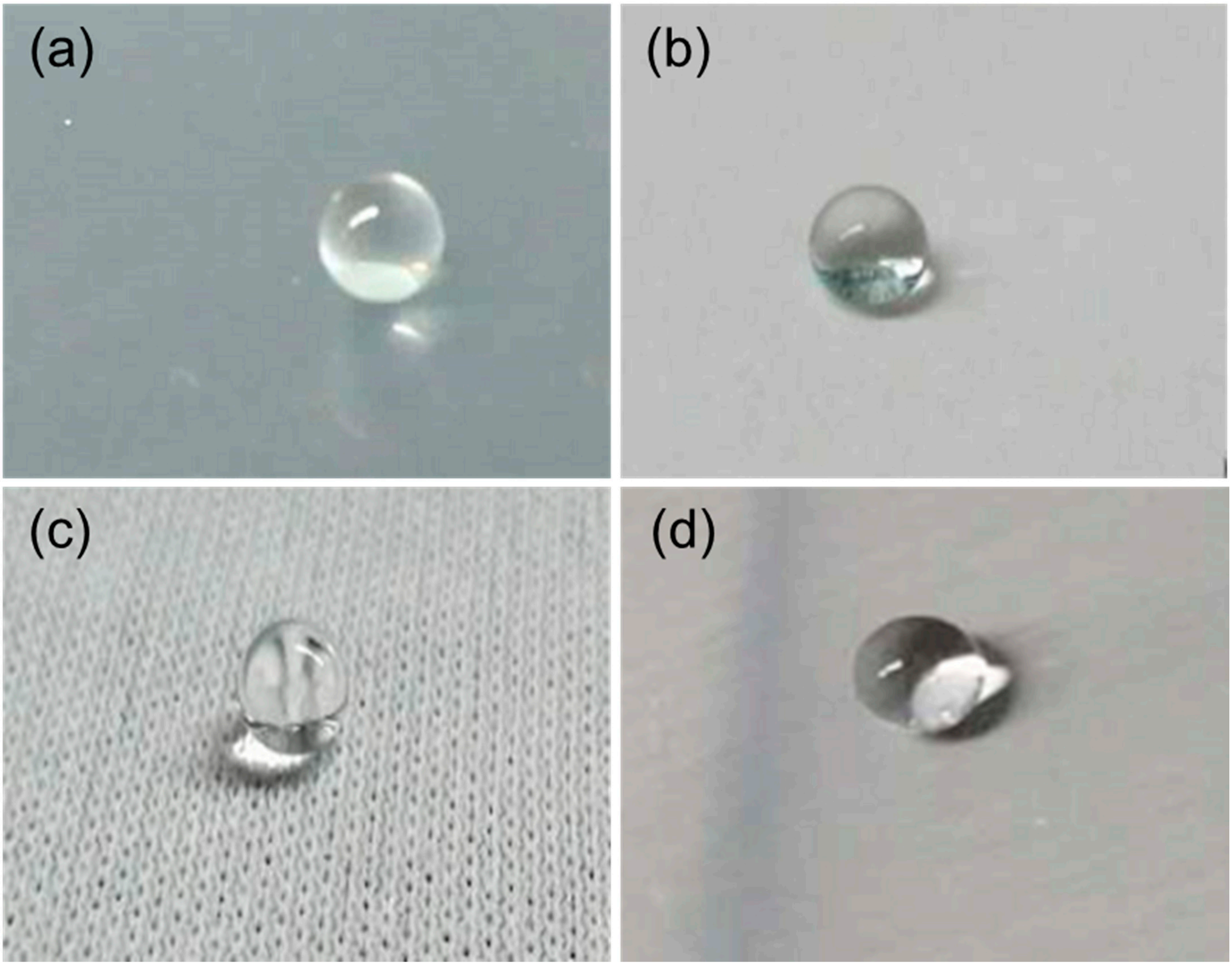

Figure 10. Optical images of spherical water droplets on different substrates, (**a**) glass, (**b**) Al_2O_3, (**c**) fabric, and (**d**) Al.

4. Conclusions

By a facile mixing and dip coating method, superhydrophobic coatings have been successfully fabricated using solutions containing SiO_2 nanoparticles, PU-166 polyurethane and ST-200 FAP. With the optimal formula used, the coating exhibits excellent hydrophobicity, with a WCA of 159° and a rolling angle of 3°. Besides, the coating has a pencil hardness of 6H and adhesion rate is 0, which demonstrate that the coating has an adequate level of mechanical strength. Moreover, the transparency and hydrophobicity of the coating was well balanced. The coating demonstrates good transparency as the optical light transmittance is 88%. Good transparency and hydrophobicity are achieved in one coating. Also, the effects of different coating components on the coating properties are systematically investigated. As the SiO_2 nanoparticles increases, the hydrophobicity of the coatings becomes higher, but the optical transmittance decreases due to the increased surface roughness. The increment of PU-166 has a positive effect on the transparency but a negative effect on the hydrophobicity of the coating, as it significantly decreases the surface roughness of the coating. As for ST-200, it has little effect on the transparency of the coating. In terms of hydrophobicity, at a low content, the addition of ST-200 improves the hydrophobicity of the coating as it lowers the surface energy of the coating. However, with an excessive amount added, the hydrophobicity is severely compromised as the ST-200 destroyed the micro/nano-scale hierarchical roughness. Overall, the fabrication is simple, requires no expensive equipment and energy consumption is reasonable. All these merits make it a suitable approach for upscale application.

Author Contributions: Conceptualization, Y.J.; methodology, Z.L., C.Z. and C.K.; resources, Z.L., C.K. and C.Z.; data curation, Z.L., C.K. and C.Z.; writing—original draft preparation, Z.L.; writing—review and editing, Z.Z., C.K., X.W. and Y.J.; supervision, Z.Z. and Y.J.; project administration, X.W. and Y.J.; funding acquisition, X.W. and Y.J. All authors have read and agreed to the published version of the manuscript.

Funding: This work was financially supported by the Dongguan Introduction Program of Leading Innovative and Entrepreneurial Talents (Grant No. 2017-16) and Guangdong Foundation and Application Research Project Regional Collaborative Funding Youth Project (Grant No. 2019A1515110537).

Informed Consent Statement: Not applicable.

Data Availability Statement: Not applicable.

Conflicts of Interest: The authors declare no conflict of interest.

References

1. Cheng, Y.; Miao, D.; Kong, L.; Jiang, J.; Guo, Z. Preparation and Performance Test of the Super-Hydrophobic Polyurethane Coating Based on Waste Cooking Oil. *Coatings* **2019**, *9*, 861. [CrossRef]
2. Safaei, M.R.; Ranjbarzadeh, R.; Hajizadeh, A.; Bahiraei, M.; Afrand, M.; Karimipour, A. Effects of cobalt ferrite coated with silica nanocomposite on the thermal conductivity of an antifreeze: New nanofluid for refrigeration condensers. *Int. J. Refrig.* **2019**, *102*, 86–95. [CrossRef]
3. Agbe, H.; Sarkar, D.K.; Chen, X. Tunable Superhydrophobic Aluminum Surfaces with Anti-Biofouling and Antibacterial Properties. *Coatings* **2020**, *10*, 982. [CrossRef]
4. Ghazali, N.; Basirun, W.J.; Nor, A.M.; Johan, M.R. Super-Amphiphobic Coating System Incorporating Functionalized Nano-Al_2O_3 in Polyvinylidene Fluoride (PVDF) with Enhanced Corrosion Resistance. *Coatings* **2020**, *10*, 387. [CrossRef]
5. Jia, L.; Sun, J.; Li, X.; Zhang, X.; Chen, L.; Tian, X. Preparation and Anti-frost Performance of PDMS-SiO_2/SS Superhydrophobic Coating. *Coatings* **2020**, *10*, 1051. [CrossRef]
6. Qian, C.; Li, Q.; Chen, X. Droplet Impact on the Cold Elastic Superhydrophobic Membrane with Low Ice Adhesion. *Coatings* **2020**, *10*, 964. [CrossRef]
7. Rasheed, T.; Shafi, S.; Bilal, M.; Hussain, T.; Sher, F.; Rizwan, K. Surfactants-based remediation as an effective approach for removal of environmental pollutants—A review. *J. Mol. Liq.* **2020**, 113960. [CrossRef]
8. Lin, Y.; Chen, H.; Wang, G.; Liu, A. Recent progress in preparation and anti-icing applications of superhydrophobic coatings. *Coatings* **2018**, *8*, 208. [CrossRef]
9. Shang, B.; Chen, M.; Wu, L. Fabrication of UV-Triggered Liquid-Repellent Coatings with Long-Term Self-Repairing Performance. *ACS Appl. Mater. Interfaces* **2018**, *10*, 31777–31783. [CrossRef]
10. Fihri, A.; Bovero, E.; Al-Shahrani, A.; Al-Ghamdi, A.; Alabedi, G. Recent progress in superhydrophobic coatings used for steel protection: A review. *Colloids Surf. A Physicochem. Eng. Asp.* **2017**, *520*, 378–390. [CrossRef]
11. Das, S.; Kumar, S.; Samal, S.K.; Mohanty, S.; Nayak, S.K. A Review on Superhydrophobic Polymer Nanocoatings: Recent Development and Applications. *Ind. Eng. Chem. Res.* **2018**, *57*, 2727–2745. [CrossRef]
12. Chen, X.; Chen, Y.; Jin, T.; He, L.; Zeng, Y.; Ma, Q.; Li, N. Fabrication of superhydrophobic coating from non-fluorine siloxanes via a one-pot sol-gel method. *J. Mater. Sci.* **2018**, *53*, 11253–11264. [CrossRef]
13. Kumar, A.; Gogoi, B. Development of durable self-cleaning superhydrophobic coatings for aluminium surfaces via chemical etching method. *Tribol. Int.* **2018**, *122*, 114–118. [CrossRef]
14. Ye, H.; Zhu, L.; Li, W.; Liu, H.; Chen, H. Simple spray deposition of a water-based superhydrophobic coating with high stability for flexible applications. *J. Mater. Chem. A* **2017**, *5*, 9882–9890. [CrossRef]
15. Şakalak, H.; Yılmaz, K.; Gürsoy, M.; Karaman, M. Roll-to roll initiated chemical vapor deposition of super hydrophobic thin films on large-scale flexible substrates. *Chem. Eng. Sci.* **2020**, *215*, 115466. [CrossRef]
16. Si, Y.; Dong, Z.; Jiang, L. Bioinspired Designs of Superhydrophobic and Superhydrophilic Materials. *ACS Cent. Sci.* **2018**, *4*, 1102–1112. [CrossRef]
17. Guo, D.; Chen, J.; Wen, L.; Wang, P.; Xu, S.; Cheng, J.; Wen, X.; Wang, S.; Huang, C.; Pi, P. A superhydrophobic polyacrylate film with good durability fabricated via spray coating. *J. Mater. Sci.* **2018**, *53*, 15390–15400. [CrossRef]
18. Ma, C.; Li, Y.; Zhang, J.; Ning, F.; Kang, M.; Li, H.; Qiu, Z. Preparation and characterization of polyacrylate composite and its application in superhydrophobic coating based on silicone-modified ZnO. *J. Coat. Technol. Res.* **2021**, 1–19. [CrossRef]
19. Hooda, A.; Goyat, M.S.; Kumar, A.; Gupta, R. A facile approach to develop modified nano-silica embedded polystyrene based transparent superhydrophobic coating. *Mater. Lett.* **2018**, *233*, 340–343. [CrossRef]

20. Latthe, S.S.; Sutar, R.S.; Shinde, T.B.; Pawar, S.B.; Khot, T.M.; Bhosale, A.K.; Sadasivuni, K.K.; Xing, R.; Mao, L.; Liu, S. Superhydrophobic leaf mesh decorated with SiO_2 nanoparticle–polystyrene nanocomposite for oil–water separation. *ACS Appl. Nano Mater.* **2019**, *2*, 799–805. [CrossRef]
21. Wei, C.; Dai, F.; Lin, L.; An, Z.; He, Y.; Chen, X.; Chen, L.; Zhao, Y. Simplified and robust adhesive-free superhydrophobic SiO_2-decorated PVDF membranes for efficient oil/water separation. *J. Membr. Sci.* **2018**, *555*, 220–228. [CrossRef]
22. Wang, M.; Liu, G.; Yu, H.; Lee, S.-H.; Wang, L.; Zheng, J.; Wang, T.; Yun, Y.; Lee, J.K. ZnO nanorod array modified PVDF membrane with superhydrophobic surface for vacuum membrane distillation application. *ACS Appl. Mater. Interfaces* **2018**, *10*, 13452–13461. [CrossRef] [PubMed]
23. Wu, Y.; Shen, Y.; Tao, J.; He, Z.; Xie, Y.; Chen, H.; Jin, M.; Hou, W. Facile spraying fabrication of highly flexible and mechanically robust superhydrophobic F-SiO_2@ PDMS coatings for self-cleaning and drag-reduction applications. *New J. Chem.* **2018**, *42*, 18208–18216. [CrossRef]
24. Deka, B.J.; Lee, E.-J.; Guo, J.; Kharraz, J.; An, A.K. Electrospun nanofiber membranes incorporating PDMS-aerogel superhydrophobic coating with enhanced flux and improved antiwettability in membrane distillation. *Environ. Sci. Technol.* **2019**, *53*, 4948–4958. [CrossRef] [PubMed]
25. Zhou, H.; Chen, R.; Liu, Q.; Liu, J.; Yu, J.; Wang, C.; Zhang, M.; Liu, P.; Wang, J. Fabrication of ZnO/epoxy resin superhydrophobic coating on AZ31 Magnesium Alloy. *Chem. Eng. J.* **2019**, *368*, 261–272. [CrossRef]
26. Ren, T.; Tang, G.; Yuan, B.; Yan, Z.; Ma, L.; Huang, X. One-step fabrication of robust superhydrophobic coatings with corrosion resistance by a self-curing epoxy-resin-based adhesive. *Surf. Coat. Technol.* **2019**, *380*, 125086. [CrossRef]
27. Ghashghaee, M.; Fallah, M.; Rabiee, A. Superhydrophobic nanocomposite coatings of poly (methyl methacrylate) and stearic acid grafted CuO nanoparticles with photocatalytic activity. *Prog. Org. Coat.* **2019**, *136*, 105270. [CrossRef]
28. Sutar, R.S.; Gaikwad, S.S.; Latthe, S.S.; Kodag, V.S.; Deshmukh, S.B.; Saptal, L.P.; Kulal, S.R.; Bhosale, A.K. Superhydrophobic Nanocomposite Coatings of Hydrophobic Silica NPs and Poly (methyl methacrylate) with Notable Self-Cleaning Ability. *Wiley Online Libr.* **2020**, *393*, 2000116. [CrossRef]
29. Luo, G.; Jin, Z.; Dong, Y.; Huang, J.; Zhang, R.; Wang, J.; Li, M.; Shen, Q.; Zhang, L. Preparation and performance enhancements of wear-resistant, transparent PU/SiO2 superhydrophobic coating. *Surf. Eng.* **2018**, *34*, 139–145. [CrossRef]
30. Yousefi, E.; Ghadimi, M.R.; Amirpoor, S.; Dolati, A. Preparation of new superhydrophobic and highly oleophobic polyurethane coating with enhanced mechanical durability. *Appl. Surf. Sci.* **2018**, *454*, 201–209. [CrossRef]
31. Zheng, H.; Pan, M.; Wen, J.; Yuan, J.; Zhu, L.; Yu, H. Robust, Transparent, and Superhydrophobic Coating Fabricated with Waterborne Polyurethane and Inorganic Nanoparticle Composites. *Ind. Eng. Chem. Res.* **2019**, *58*, 8050–8060. [CrossRef]
32. Yu, N.; Xiao, X.; Ye, Z.; Pan, G. Facile preparation of durable superhydrophobic coating with self-cleaning property. *Surf. Coat. Technol.* **2018**, *347*, 199–208. [CrossRef]
33. Huang, J.; Lyu, S.; Chen, Z.; Wang, S.; Fu, F. A facile method for fabricating robust cellulose nanocrystal/SiO_2 superhydrophobic coatings. *J. Colloid Interface Sci.* **2019**, *536*, 349–362. [CrossRef] [PubMed]
34. Yang, M.; Liu, W.; Jiang, C.; He, S.; Xie, Y.; Wang, Z. Fabrication of superhydrophobic cotton fabric with fluorinated TiO_2 sol by a green and one-step sol-gel process. *Carbohydr. Polym.* **2018**, *197*, 75–82. [CrossRef] [PubMed]
35. Kokare, A.M.; Sutar, R.S.; Deshmukh, S.G.; Xing, R.; Liu, S.; Latthe, S.S. *ODS–Modified TiO_2 Nanoparticles for the Preparation of Self-Cleaning Superhydrophobic Coating*; AIP Publishing LLC: Melville, NY, USA, 2020; p. 100068. [CrossRef]
36. Hwang, G.B.; Patir, A.; Page, K.; Lu, Y.; Allan, E.; Parkin, I.P. Buoyancy increase and drag-reduction through a simple superhydrophobic coating. *Nanoscale* **2017**, *9*, 7588–7594. [CrossRef]
37. Sun, K.; Liu, H.; Wang, X.; Wu, D. Innovative design of superhydrophobic thermal energy-storage materials by microencapsulation of n-docosane with nanostructured ZnO/SiO_2 shell. *Appl. Energy* **2019**, *237*, 549–565. [CrossRef]
38. Satapathy, M.; Varshney, P.; Nanda, D.; Mohapatra, S.S.; Behera, A.; Kumar, A. Fabrication of durable porous and non-porous superhydrophobic LLDPE/SiO_2 nanoparticles coatings with excellent self-cleaning property. *Surf. Coat. Technol.* **2018**, *341*, 31–39. [CrossRef]
39. Radwan, A.B.; Abdullah, A.M.; Hassan, M.K. The missing piece of the puzzle regarding the relation between the degree of superhydrophobicity and the corrosion resistance of superhydrophobic coatings. *Electrochem. Commun.* **2018**, *91*, 41–44. [CrossRef]
40. Vu, M.C.; Bach, Q.-V.; Nguyen, D.D.; Tran, T.S.; Goodarzi, M. 3D interconnected structure of poly (methyl methacrylate) microbeads coated with copper nanoparticles for highly thermal conductive epoxy composites. *Compos. Part B Eng.* **2019**, *175*, 107105. [CrossRef]
41. Karimipour, A.; Bagherzadeh, S.A.; Goodarzi, M.; Alnaqi, A.A.; Bahiraei, M.; Safaei, M.R.; Shadloo, M.S. Synthesized $CuFe_2O_4$/SiO_2 nanocomposites added to water/EG: Evaluation of the thermophysical properties beside sensitivity analysis & EANN. *Int. J. Heat Mass Transf.* **2018**, *127*, 1169–1179. [CrossRef]
42. Alrashed, A.A.A.A.; Karimipour, A.; Bagherzadeh, S.A.; Safaei, M.R.; Afrand, M. Electro-and thermophysical properties of water-based nanofluids containing copper ferrite nanoparticles coated with silica: Experimental data, modeling through enhanced ANN and curve fitting. *Int. J. Heat Mass Transf.* **2018**, *127*, 925–935. [CrossRef]